ACI STRUCTURAL JOURNAL TECHNICAL PAPER

Title no. 108-S39

Seismic Strengthening of Infilled Reinforced Concrete Frames with Composite Materials

by Sevket Ozden, Umut Akguzel, and Turan Ozturan

The overall performance of hollow clay tile infilled reinforced concrete (RC) frames strengthened with carbon fiber-reinforced polymer (CFRP) materials is experimentally investigated in this paper. For this purpose, five one-third scale, one-bay, two-story specimens were constructed with common deficiencies (that is, low concrete strength, insufficient lap splice length, poor confinement, and lack of joint reinforcement) observed in existing RC frames and tested under reversed cyclic lateral loading. The test results indicated that the investigated strengthening schemes yielded a significant enhancement in both the response and the load capacity. It is also seen that the effectiveness of the strengthening strongly depends on the composite action of the infill panel, ensuring that the surface-bonded fiber-reinforced polymer (FRP) is provided with a sufficient anchorage development length to the surrounding frames. Results and discussions are presented on the basis of the observed global performance and local failure mechanisms along with the detailed comparisons of similar studies. Conclusions are also drawn to provide tentative retrofit FRP scheme recommendations.

Keywords: fiber-reinforced polymer; loading; rehabilitation; reinforced concrete; strength.

INTRODUCTION

Recently, fiber-reinforced composites have attracted considerable attention for the seismic strengthening of existing structures. In addition to their advanced mechanical properties, ease of in-place application, and savings in construction cost and time can account for their appealing properties in retrofit applications. Numerous studies have been carried out in the last decade on the use of fiber-reinforced polymer (FRP) materials in concrete structures.

Most of the specimens tested in various laboratories represented a small scale of prototypes and were conducted through the strengthening of individual reinforced concrete (RC) members or brick walls. The majority of the work conducted to date related to brick-wall strengthening has been on the out-of-plane response of walls with externally bonded FRP. Other variations between the experimental investigations are the types of FRP materials used and subsequently their mechanical characteristics. Some of the research involving the out-of-plane and in-plane behavior of brick walls can be found in the literature.[1-7]

It is well known from field reports and observations that unreinforced masonry infills in existing RC structures make a significant contribution to the disastrous consequences of earthquakes. To address this problem, few studies have been conducted on the strengthening methods for nonductile existing RC structures with infilled masonry panels using carbon fiber-reinforced polymer (CFRP) strips. For the sake of completeness, the previous research on this topic is briefly summarized in the following section. Further information on the conventional strengthening methods of RC frames can be found in Sugano.[8]

SUMMARY OF RELEVANT RESEARCH

In 2003, a comprehensive experimental campaign within the framework of a North Atlantic Treaty Organization (NATO) project commenced and was led by Middle East Technical University (METU) in collaboration with three other national institutions: Istanbul Technical University (ITU), Kocaeli University (KU), and Bogazici University (BU), along with the contributions of institutions from abroad.[9] The aim was to develop efficient, economical, and easily applicable strengthening techniques for existing nonductile RC frames in Turkey. The types and dimensions of the test specimens and loading schemes used in this research are comparable with those tested by METU and ITU. Different patterns, amounts, and anchorage types of CFRP sheets were among the studied parameters. For the sake of comparison and to draw conclusions, the studied parameters and outcomes from the METU and ITU test campaigns are briefly explained in the following sections.

At METU,[10] a total of seven specimens were constructed and tested with lap splices in the second story. Transverse reinforcement in the provided lap splice region did not comply with Turkish Seismic Design Code requirements, although the lap splice length was adequately employed according to the code requirements. The first infilled specimen, Specimen SP-1, was tested as a benchmark. Limited lateral load and displacement capacities were observed due to first-story beam-column joint shear failure. The maximum load attained was 55 kN (12.4 kips). The second specimen, Specimen SP-2, was strengthened by covering both faces with one-directional CFRP sheets (blanket-type application) without any connection to the surrounding frame members. Debonding from the plastered surface occurred at the early stages of the test due to no extension or anchorage being provided to the frame. The specimen failed in the same fashion as Specimen SP-1. In Specimen SP-3, only the exterior face of the infill was fully covered by two orthogonal CFRP sheets (blanket-type application) and they were anchored to the frame members by special anchors. The failure of an anchor located at the midheight of the second-story columns initiated the delamination of the CFRP layers on the second-story infill panel. The peak load attained by the specimen was 65.4 kN (14.7 kips). A blanket-type application scheme was used in Specimen SP-4 with an extension of CFRP

ACI Structural Journal, V. 108, No. 4, July-August 2011.
MS No. S-2009-289.R1 received June 2, 2010, and reviewed under Institute publication policies. Pertinent discussion including author's closure, if any, will be published in the May-June 2012 *ACI Structural Journal* if the discussion is received by January 1, 2012.

Sevket Ozden *is an Associate Professor in the Civil Engineering Department at Kocaeli University, Kocaeli, Turkey. He received his BSc from Bogazici University, Istanbul, Turkey; his MASc from the University of Toronto, Toronto, ON, Canada; and his PhD from Bogazici University. His research interests include the strengthening of reinforced concrete members and frames and the connection performance of precast structures.*

Umut Akguzel *is a PhD Candidate and Research Assistant in the Department of Civil and Natural Resources Engineering at the University of Canterbury, Christchurch, New Zealand. He received his MSc from Bogazici University. His research interests include the rehabilitation of reinforced concrete and masonry structures using advanced composite materials, the analysis of repaired and rehabilitated reinforced concrete structures, and performance-based seismic design.*

ACI member **Turan Ozturan** *is a Professor of civil engineering in the Department of Civil Engineering at Bogazici University. His research interests include cement composites, high-performance concretes, use of mineral admixtures in concrete, and concrete durability.*

sheets to the frame members. The lateral load capacity was significantly increased to 131.5 kN (29.6 kips). Governing the failure modes were the buckling of CFRP overlays at the edge of the first-story joint and the anchorage failure at the bottom of the first-story column, along with a complete delamination at the foundation level. In Specimen SP-5, CFRP strips were placed in a cross-bracing configuration to decrease the amount of CFRP used and were anchored to the frame and infills, as in Specimen SP-4. Specimen SP-5 failed due to the buckling of the CFRP material in the compression strut, followed by failure of the anchor dowels at the foundation level. The lateral load capacity (118 kN [16.5 kips]) and energy dissipation properties were quite similar. In Specimen SP-6, the plastic hinge zones at the base of the first-story columns were also confined in addition to Specimen SP-5's strengthening scheme. The behavior, however, did not improve. Following the sudden failure of anchors of the tensile strut, brittle shear failure in the first-story beam-column joint occurred. The maximum lateral load capacity was 100 kN (22.4 kips). The size of the anchors was increased in Specimen SP-7. A similar global performance to that of Specimen SP-6, however, was observed.

At ITU,[11] a total of seven 1/2-scale models of nonductile frames with a similar configuration (that is, a two-story, one-bay configuration) were tested. For reference, four benchmark specimens, namely Specimens BL-0-1.8.6 (bare frame with deficient lap splice), IL-0-1-17 (infilled frame with deficient lap splice), BC-0-1.8.6 (bare frame with continuous longitudinal reinforcement), and IC-0-1-17 (infilled frame with continuous longitudinal reinforcement) were tested. In general, nonductile failure modes were observed. In the bare frames, shear failure in the joints and damage accumulation in the lower parts of the first-story columns occurred, whereas in the infilled frames, spread of bending cracks along the columns and corner crushing of the infilled specimens was observed. The maximum attained lateral load capacities of these specimens were 27.7, 185, 40.4, and 165 kN (6.2, 41.6, 9, and 37 kips) for Specimens BL-0-1.8.6, IL-0-1-17, BC-0-1.8.6, and IC-0-1-17, respectively. Specimens IL-C1-1-10 (with deficient lap splice) and IC-C1-1-10 (with continuous longitudinal reinforcement) were strengthened with a one-ply CFRP sheet on two sides of the frame. CFRP fabrics were applied in both diagonal directions on both sides of the infills by means of anchors and at the corners of the panels with additional CFRP fabrics (flag sheets). CFRP strips were applied in the vertical direction on the sides of the column along with confinement of the column to eliminate lap splice deficiency. The last specimen, Specimen IC-C2-1-22, was strengthened in a similar fashion, where CFRP was applied only on one side. Specimens IL-C1-1-10 and IC-C1-1-10 experienced fracture of the diagonal fabric under tension at a drift ratio of 0.8%. The lateral load capacities of the retrofitted specimens were 221, 258, and 271 kN (50, 58, and 61 kips) for Specimens IC-C1-1-10, IL-C1-1-10, and IC-C2-1-22, respectively.

Saatcioglu et al.[12] also studied the seismic performance of an RC frame infilled with concrete block masonry. Two 1/2-scale, one-bay, one-story specimens were tested with and without seismic retrofitting using CFRP sheets bonded on the surface of masonry wall and anchored to the surrounding frame with CFRP anchor dowels. The test results showed that the CFRP sheets controlled cracking and increased lateral bracing, improving the elastic capacity of the system. An increase in lateral force resistance of approximately 300% was observed.

An experimental study has recently been presented in the literature[13] investigating the effect of CFRP strip width (that is, 200, 300, and 400 mm [7.87, 11.81, and 15.75 in.]) and application type (that is, interior, exterior, and both sides of the masonry wall) on the seismic strengthening of RC infilled frames with CFRP overlays. A total of ten 1/3-scale, one-bay, one-story nonductile specimens were tested. CFRP strips were applied symmetrically to the infill walls and anchored to both the infill wall and the RC frame. The test results showed that the load capacity increased by nearly 2.5 times when both sides of the walls had CFRP applied when compared to a one-sided application. It was also indicated, however, that an increase in the width of the CFRP strip has a limited effect on the enhancement of strength and stiffness.

RESEARCH SIGNIFICANCE

The pre-earthquake seismic strengthening of the existing hollow clay tile infilled nonductile RC frames with CFRP cross overlays, bonded to the existing brick walls and anchored to the surrounding frame, is a relatively novel technique in comparison to the introduction of new cast-in-place RC shear walls. Strengthening with CFRP overlays needs to be investigated to highlight the attainable strength enhancement and failure mechanisms along with the applicability of the retrofit technique. Knowledge gained from this study can be used to refine the existing models and pave the way for economically feasible rehabilitation techniques.

EXPERIMENTAL PROCEDURE

Test specimens

Five 1/3-scale, one-bay, two-story RC frames were designed and constructed with seismically deficient characteristics, similar to the existing midrise RC frame structures.[14] The benchmark specimens consisted of one bare frame (Specimen B) and one hollow clay tile infilled frame (Specimen I). The remaining three specimens were named according to their retrofitting scheme type: 1) Specimen IX was the infilled frame retrofitted by CFRP cross overlays on the masonry panel; 2) Specimen IXF had additional flag sheets on the corner of the infill panels in addition to the same CFRP cross overlay scheme used in Specimen IX; and 3) Specimen IXFC was retrofitted using the same overlay scheme of Specimen IXF with the additional CFRP confinement of the columns. CFRP cross overlays and flag sheets were anchored into the foundation and surrounding frame elements. CFRP anchorage depths were also modified in each retrofit scheme to devise a useful development length to provide sufficient anchorage to the surrounding frame. More detailed information on the CFRP application procedure and detailing are given in the specimen fabrication section.

Table 1—Summary of test results

Specimen	Specimen description	f'_c, MPa (ksi)	f'_m, MPa (ksi)	P_{cr}, kN (kips)	P_y, kN (kips)	P_{max}, kN (kips)	Drift at P_{max}, %	Governing failure mechanism
B	Bare frame	15.0 (2.2)	—	7 (1.6)	10.0 (2.3)	11.7 (2.5)	1.00	Flexural failure in columns and beam-column joint shear failure (first story)
I	Infilled frame	15.0 (2.2)	5.5 (0.8)	40 (7.9)	55 (12.7)	59.3 (13.3)	0.21	Failure in infill compression strut resulting infill panel corner crushing
IX	Infilled frame retrofitted with cross overlay	16.0 (2.3)	5.0 (0.7)	35 (8.9)	74.6 (17.2)	75 (16.9)	0.25	Corner crushing, CFRP buckling, and anchorage failure at the foundation
IXF	IX type of retrofit plus flag sheet	15.0 (2.2)	3.7 (0.5)	55 (12.4)	90 (20.7)	93 (20.9)	0.34	Sliding and rocking at foundation level due to the CFRP anchorage failure
IXFC	IXF type of retrofit plus column confinement and continuity strips	14.5 (2.1)	4.7 (0.7)	55 (12.4)	100.7 (23.2)	114 (25.6)	0.93	Brittle sliding shear plane above column confinement level

Identical reinforcing schemes and poor construction practices were employed in all specimens. The dimensions and reinforcement details are given in Fig. 1. Column longitudinal bars were spliced at the foundation and first-story levels with a lap length of $20D_b$. Moreover, inadequate beam and column transverse reinforcement with 90-degree hooks was used in the beams and columns. The beams were designed stronger than the columns and there were no ties at the beam-column joints. The yield strength of the longitudinal and transverse steel was f_y = 380 MPa (55 ksi) and f_{yw} = 241 MPa (35 ksi), respectively.

Material properties

To simulate low-quality concrete, the targeted concrete compressive strength was f'_c = 15 MPa (2.2 ksi). Specially fabricated, scaled-down, hollow clay tiles (70 x 85 x 90 mm [2.8 x 3.3 x 3.5 in.]) were used as infill. The tile dimension perpendicular to the plane of infill was 70 mm (2.8 in.). Low-strength mortar was used in brick masonry and for plastering both faces of the frame. The concrete and mortar compressive strengths taken from 150 x 300 mm (6 x 12 in.) cylinders and 50 mm (1.9 in.) cubes are given in Table 1. The CFRP material used for strengthening was a unidirectional continuous fabric. The mechanical properties of the cured laminate with epoxy, as provided by the manufacturer, are as follows: tensile E-modulus E_f = 65,402 MPa (9487 ksi), tensile strength f_{uf} = 894 MPa (129.7 ksi), failure strain ε_{fu} = 1.33%, and ply thickness t_f = 0.381 mm (0.015 in.). On the other hand, the manufacturer-provided mechanical properties of the fiber itself are as follows: E_f = 231,000 MPa (33,502 ksi), f_{uf} = 4100 MPa (594.6 ksi), ε_{fu} =1.7%, and t_f = 0.120 mm (0.0047 in.). The epoxy-based impregnating resin, which was also used as a seal coat during the application, has a modulus of elasticity of E_e = 3800 MPa (551 ksi) and a tensile strength of f_e = 30 MPa (4.4 ksi).

Specimen fabrication and strengthening

As mentioned previously, all details of the hollow clay tile infilled frame specimens, including the width of CFRP cross overlay and orientation, were the same, except for the particular anchorage applications (Fig. 2). To demonstrate the actual application in practice, frames and infills were constructed by professional construction workers. Hollow clay tiles were laid in such a way that the direction of the tile holes was parallel to the columns' longitudinal direction. Following the brick infill construction, both sides of the test specimens were also plastered. The plaster thickness on either side was approximately 7 to 8 mm (0.28 to 0.32 in.). On one side of the frame (designated as the back face herein), the brick infill was on the same plane as the column face.

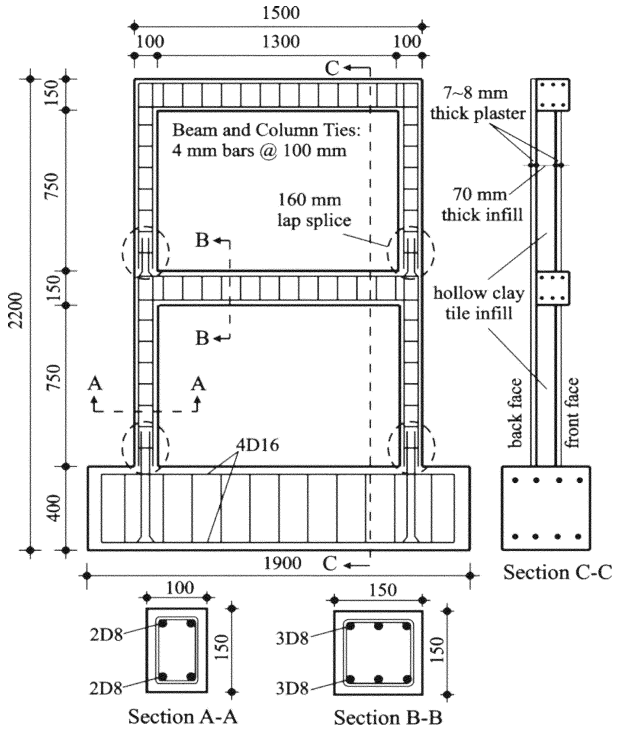

Fig. 1—Details of test specimens. (Note: Dimensions in mm; 1 mm = 0.0394 in.; nominal diameter of bars: D4 = 4 mm, D8 = 8 mm, and D16 = 16 mm.)

In all retrofitted specimens, CFRP overlays were placed to work as cross-diagonal struts anchored to the RC frame and to the counterpart overlay on the opposite infill face through CFRP dowels. Specimen IX was the first infilled frame strengthened through the application of CFRP cross-diagonal overlays only, having equal widths of w = 200 mm (7.9 in.) on both faces of the brick infill (Fig. 2).

Flag sheets were added in the corner of the infill panels in all stories of Specimens IXF and IXFC, along with the CFRP cross overlay application, similar to that of Specimen IX. In Specimen IXFC, columns in the base and first-story level were confined. Continuity strips were also applied in Specimen IXFC between the first- and second-story columns, along with the first-story column and the foundation, which was anchored to the foundation at the external sides of the base-level columns. Because the carbon fibers were unidirectional, flag sheets were applied by laying two layers of fabric in both the horizontal and vertical directions, whereas confinement overlays were only horizontal and continuity strips were only vertical (Fig. 2).

Any dust or loose particles on the frame or in the anchor holes were removed before the application of epoxy resin by

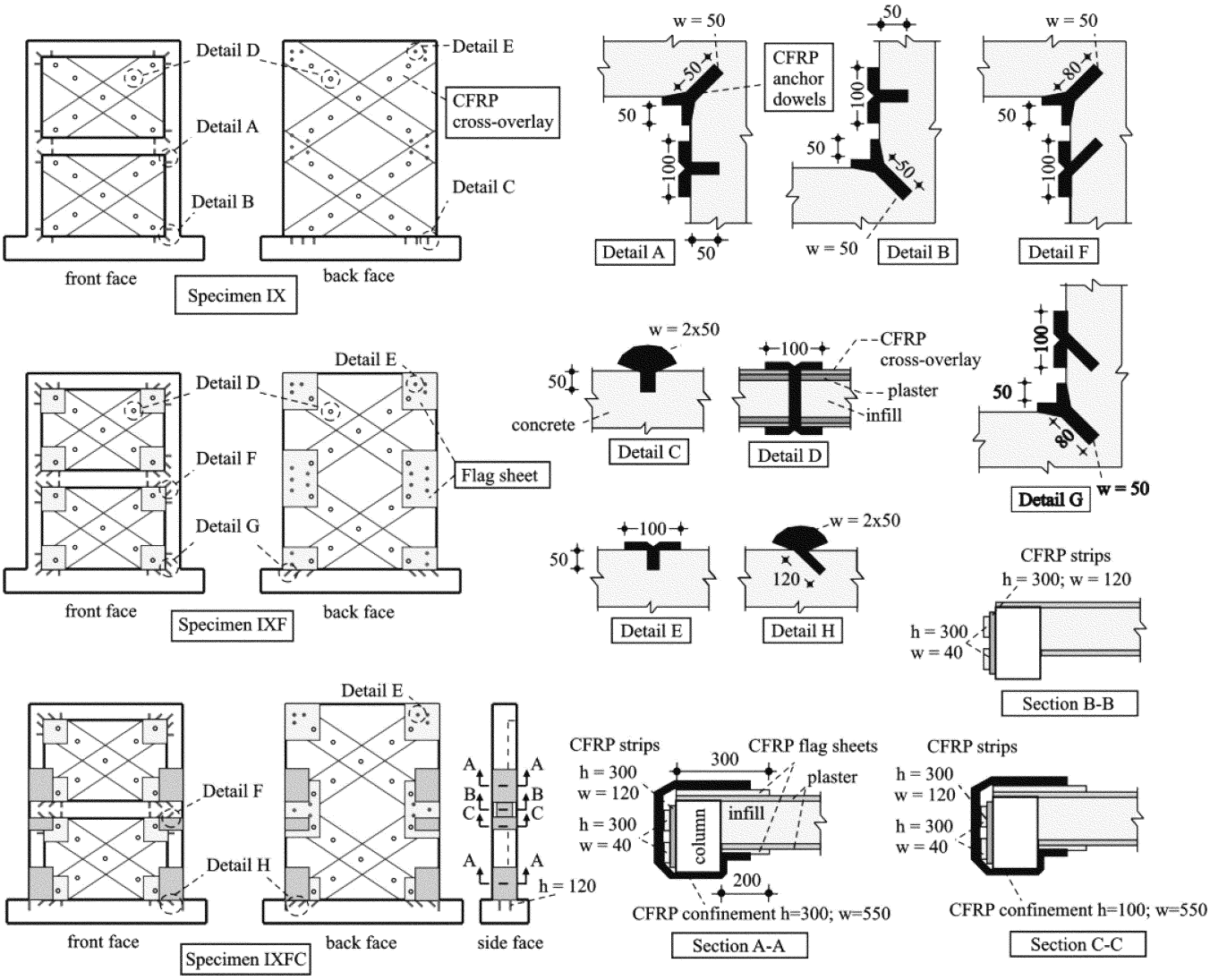

Fig. 2—Schematic view of CFRP arrangement and anchorage details. (Note: Dimensions in mm; 1 mm = 0.0394 in.; w *and* h *are width and height, respectively.)*

means of an industrial vacuum cleaner. The column corners of Specimen IXFC were rounded to a radius of 10 mm (0.4 in.) before the application of the confining CFRP overlays. A two-component epoxy resin was applied to the prepared specimen surfaces using a trowel and brush before the application of fiber sheets. Afterward, carbon fiber sheets—cut to predetermined dimensions—were placed onto the resin and carefully applied to the surface via a laminating roller until the epoxy was squeezed out between the roving. Epoxy-saturated CFRP anchor dowels were plugged into the holes by means of tie wires and during the placement, epoxy resin was initially injected into the holes. The ends of the anchor dowels remaining outside the holes, either in the brick infill or the RC frame, were glued to CFRP sheets for proper anchorage. The dimensions of the anchor dowels were slightly changed in Specimens IX, IXF, and IXFC. The width of the anchor dowels was 2 x 50 mm (2 x 2 in.) and the diameter of the holes was 12 mm (0.5 in.) for all specimens (Fig. 2).

Test setup and loading protocol

The test setup consisted of a strong floor, a reaction wall, lateral and vertical loading systems, and an out-of-plane displacement restraining frame (Fig. 3). Lateral load was applied with a 250 kN (56.3 kips) capacity hydraulic actuator. For the bare frame, the horizontal cyclic loading was applied at the second-story beam level. The lateral load was divided into two by a steel spreader beam and applied at both the first- and second-story beam levels to the brick-infilled specimens in such a way that two-thirds of the applied load went to the upper story. The column axial load, which was applied by means of a vertical-load-distributing beam to the columns, was kept constant at a level of approximately 10% of the columns' axial capacity (N = 2 x 30 kN [2 x 6.8 kips]). A two-phase reversed cyclic loading scheme was used in the experiments. The load level was increased by increments of 5 kN (1.1 kips) in the elastic response range, whereas a deformation-controlled loading scheme was applied during the nonlinear response cycles. Loading in one direction and then unloading constituted half a cycle. Each test continued until the specimen experienced a significant loss of capacity.

An electronic data acquisition system with control feedback was used to measure the level of applied load and the in-plane lateral displacements. Two strain-gauge-based linear variable differential transducers (LVDTs) were mounted on each floor level to measure the average story displacement. For

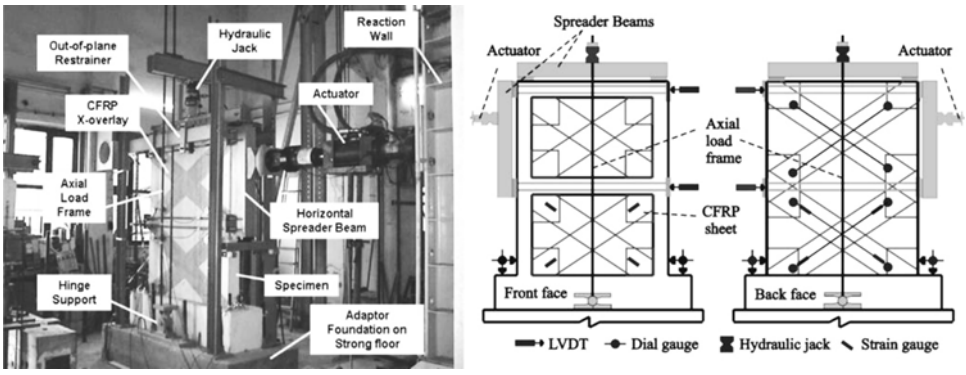

Fig. 3—Test setup and schematic view of instrumentation.

the infill specimens, shear deformations on the brick infill, horizontal base slip, and frame base rocking were also measured by LVDTs. All measurements were relative to the frame foundation. Strain gauges were also attached to the CFRP cross overlays in the last specimen (Specimen IXFC) to determine the attained strain level. The instrumentation arrangement is given in Fig. 3.

EXPERIMENTAL RESULTS AND DISCUSSION

Behavior and damage propagation

The response of Specimen B (as-built RC bare frame) displayed typical nonductile frame behavior (Fig. 4(a)). Beam-column joints failed in shear due to the lack of joint ties, and the column ends at the lap splice regions experienced plastic hinging. Hairline cracks were formed at 0.37% drift (9.5 kN [2.1 kips]) in the first-story level beam-column joints. Note that drift is defined as the ratio of lateral displacement at the second-story beam level to the height of the frame. The specimen reached its yielding capacity at 0.45% drift (10 kN [2.25 kips]). The lateral load of the specimen stabilized under the increasing lateral displacements until the end of the test.

Specimen I (as-built RC infilled frame) exhibited a combination of flexure and relative sliding and crushing of the infill panel in the compression regions (Fig. 4(b) and 5(a)). At 0.35% drift, sliding was observed between the first-story infill and the first-story beam. At increasing drift levels, separation of plaster and crushing of the infill along the compression struts was observed, while the number of cracks in the columns increased. Between 0.55% drift (40 kN [9 kips]) and 0.70% drift (36 kN [8 kips]), no new cracks formed. At these drift levels, the tip of the compression struts started to crush in the first-story infill panel. The test was terminated at a drift level of 1.1%.

In Specimen IX (retrofitted with only CFRP cross overlays), flexural cracks started to develop in the lap splice regions of the first-story left and right columns after 0.03% drift (40 kN [9.0 kips]). Following the 0.06% drift (55 kN [12.4 kips]), new flexural cracks were observed around the column tension sides. At 0.10% drift (65 kN [14.6 kips]), previously formed column flexural cracks extended through the first-story infill panels and stabilized after 0.25% drift (75 kN [17 kips]). CFRP debonding started at the foundation level, along with the sliding at the interface of the second-story panel and the first-story top beam at 0.31% drift (65 kN [14.6 kips]) (Fig. 4(c) and 5(b)). Simultaneous fracture of the CFRP overlay on the corners of the first-story infill panel and anchorage failure at the column lap splice region happened at 0.65% drift (54 kN [12.2 kips]). At approximately

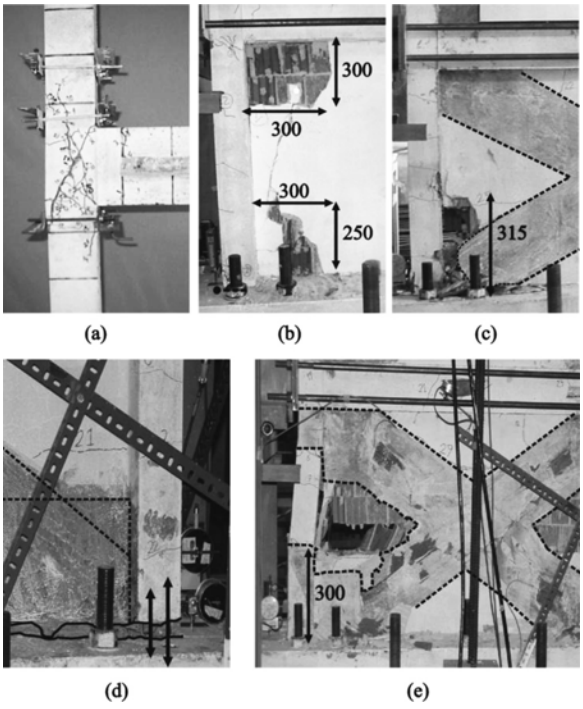

Fig. 4—Close-up views of local failures: (a) Specimen B; (b) Specimen I; (c) Specimen IX; (d) Specimen IXF; and (e) Specimen IXFC. (Note: Dimensions in mm; 1 mm = 0.0394 in.)

1.0% drift (71 kN [16 kips]), the CFRP sheets at the first-story panel started to debond and buckled in compression. The test was terminated at 1.56% drift (56 kN [12.6 kips]) after the observed drastic drop in bearing capacity due to pullout cone failure of the CFRP anchor dowels at the foundation level.

Flexural hairline cracks developed in the first-story left columns of Specimen IXF (retrofitted with CFRP cross overlays and flag sheets) approximately 200 mm (7.9 in.) above the foundation level at 0.034% drift (55 kN [12.4 kips]). In the following cycles—up to 0.089% drift (80 kN [18.0 kips])—flexural cracks continued to develop and encircle the first-story columns. Yielding of the specimen was observed upon the formation of the boundary separation between the frame and first-story infill at 0.11% drift (90 kN [20.3 kips]). At 0.34% drift (93 kN [20.9 kips]), preformed cracks, especially those on the bottom of the columns, started to widen suddenly and reached a 4 mm (0.15 in.) crack width. During the further increase of drift levels, the separation of the frame base and the frame foundation was more pronounced due to the complete loss of CFRP anchorage and excessive slip in

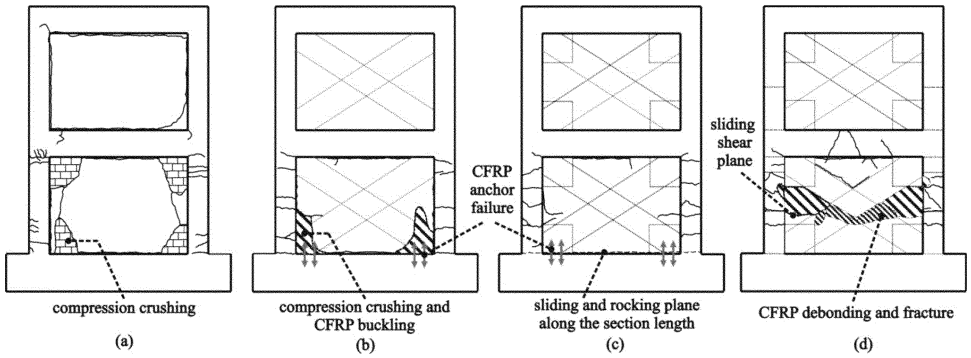

Fig. 5—Observed damage after testing: (a) Specimen I; (b) Specimen IX; (c) Specimen IXF; and (d) Specimen IXFC.

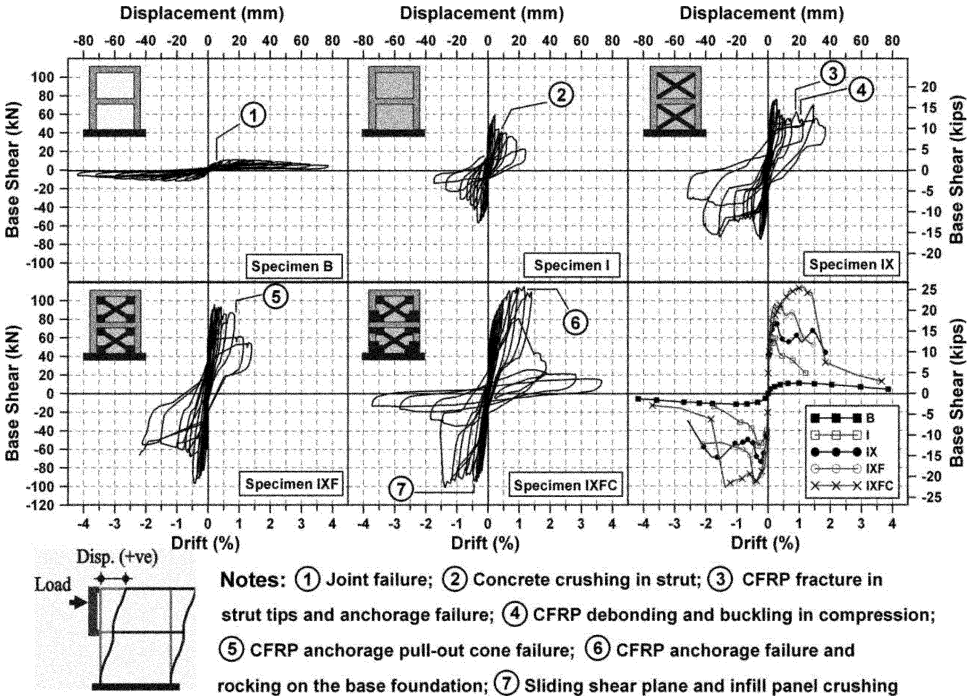

Fig. 6—Lateral load-displacement hysteresis loops and backbone curves. (Note: Dimensions in mm; 1 mm = 0.0394 in.)

the column longitudinal bars (Fig. 4(d) and 5(c)). The test was terminated at 1.05% drift (55 kN [12.4 kips]).

In Specimen IXFC (retrofitted with CFRP cross overlays, flag sheets, continuity reinforcement, and confinement in the columns), the first visible crack was observed at 0.05% drift (55 kN [12.4 kips]) above the first-story CFRP column wrap on the left column. In the following cycles, up to 0.37% drift (95 kN [21.4 kips]) beam-panel interface cracks continued to extend, along with the formation of new flexural cracks adjacent to the CFRP column wrap. At 0.37% drift, debonding and peeling suddenly occurred on the cross overlay CFRP sheets. Boundary separation between the frame and the brick infill wall also transpired in the first story. A sliding shear plane formed along the first-story wall panel above the column CFRP confinement (Fig. 4(e) and 5(d)), extending through the CFRP cross overlay and causing a sudden rupture at 0.93% drift (114 kN [25.7 kips]). The test was terminated at 3.27% drift (15 kN [3.4 kips]).

Strength and stiffness

One of the most important factors that determines the effectiveness of a seismic strengthening technique is the enhancement achieved in the lateral load-carrying capacity of the structure. The test results showed that the lateral load capacities of all strengthened frames are significantly higher than that of the bare frame, Specimen B, as well as the nonstrengthened infilled frame, Specimen I. Although there was a significant strength enhancement in Specimen IXFC (1.94 times that of Specimen I), the improvement in displacement capacity was more pronounced (5.3 times that of Specimen I). A comparison of the envelope curves (Fig. 6) indicates that the roof displacement capacity at failure of the strengthened specimens (Specimens IX to IXFC) was successively increased with the changing strengthening scheme. For instance, the peak loads of Specimens I, IX, and IXF were reached at drift ratios of 0.21%, 0.25%, and 0.34%, respectively, whereas the drift ratio at peak load of Specimen IXFC reached 0.93%, which clearly demonstrates the

changing effectiveness of different CFRP strengthening schemes on performance. The test results also indicated that the limiting interstory drift ratio for the ultimate load of the strengthened frames (Specimens IX and IXF) can be taken as 0.35%. A summary of the test results is presented in Table 1; the load-displacement hysteresis curves are shown in Fig. 6.

The degradation of normalized peak-to-peak stiffness (the ratio of stiffness of the *i*-th cycle to the stiffness of the first cycle) with corresponding drift ratios is presented in Fig. 7. The slope of the line connecting the positive and negative maximum load points of the specific cycle of the load-displacement curve was defined as the stiffness of this cycle. In general, it was observed that stiffness degradation is relatively high at small drift levels. In particular, failure of the infill panels at the first-story level resulted in a sudden drop of stiffness until the roof drift reached approximately 0.5%. Moreover, the stiffness degradation of all specimens is stabilized beyond a drift ratio of approximately 1.0%. On the other hand, Specimens I, IX, and IXF behaved similarly after the 0.5% drift level. It is also noteworthy that, although the initial stiffness and the lateral load-bearing capacity of the bare frame was the lowest among the specimens, stiffness degradation of that specimen progressed at a relatively slow rate. The peak-to-peak stiffness values of the infilled specimens (Specimens I to IXFC), regardless of the strengthening scheme, are comparable for the initial load cycles.

Energy dissipation characteristics

The total amount of dissipated hysteretic energy is a property that has long been recognized to be of paramount importance with respect to the seismic performance of a structure. The energy dissipation capacity of the test specimens under reversed cyclic loading is defined as the area enclosed by the experimental load-displacement hysteresis loops in this study. In addition, energy dissipation is also represented by the equivalent damping ratio, which is defined as the energy dissipated during a complete loading cycle normalized by the elastic energy stored in the member at a given drift level.[15] It is obvious that the larger the area of the hysteresis loop, the larger the dissipated energy; hence, the damping effect will be larger. The cumulative dissipated energy values for each specimen are given in Table 1.

As shown in Fig. 8, all specimens except the bare-frame specimen (Specimen B) dissipated almost the same amount of energy up to the 3.5% cumulative roof drift ratio. Although the dissipated energy in the last cycles of Specimen IXF was lower than Specimen IX, they dissipated almost the same amount of energy, up to a 7.5% cumulative roof drift ratio. During the 10% cumulative roof drift ratio, Specimen IXFC had the ability to dissipate approximately 1.15 times the energy dissipated by Specimen IXF. Table 1 shows the cumulative energy dissipated by all specimens until the end of the test. Note that the difference in the global behavior (that is, rocking of the rigid upper block on the frame foundation) led to 30% less energy dissipation in Specimen IXF compared to Specimen IX.

The equivalent viscous damping ratio curves are also given in Fig. 8. It is observed that, although high values were observed for cumulative roof drift ratios smaller than 2%, a drastic drop is observed between 2 and 5% for almost all specimens. The damping ratios gradually increased, especially after experiencing a 5% cumulative roof drift ratio. Note that the cumulative roof drift ratio is calculated by summing up

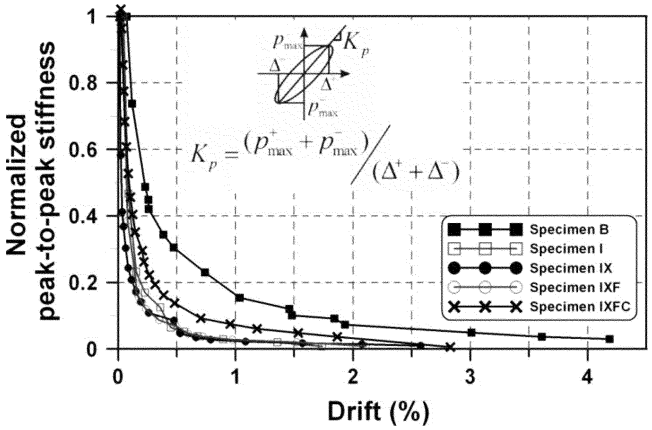

Fig. 7—Normalized peak-to-peak stiffness versus imposed drift ratio.

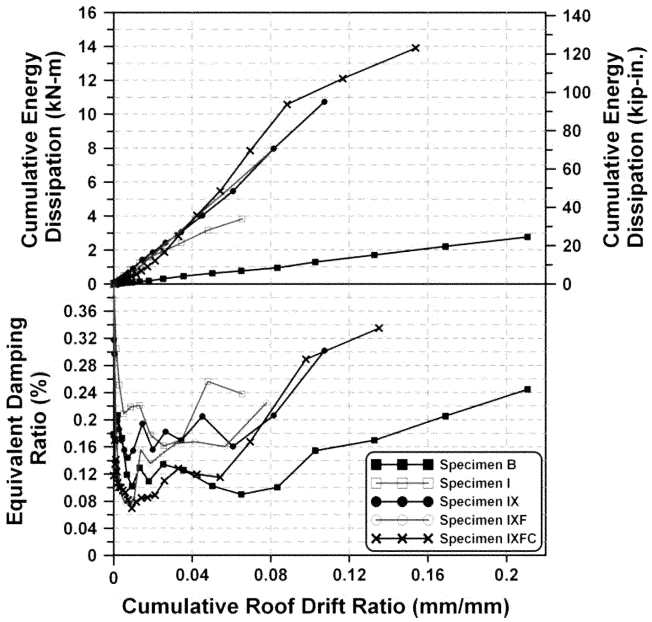

Fig. 8—Comparison of energy dissipation characteristics: cumulative energy dissipation and equivalent viscous damping curves.

the roof displacements applied during the test until that specific load cycle.

Strains of CFRP cross overlays

In Specimen IXFC, the strain values in the CFRP cross overlays of the first-story panel were measured by four strain gauges—two on the back face and two on the front face (Fig. 9). An effective diagonal FRP strain level of approximately 0.002 to 0.003 was recorded in the case of anchor failure mode by the previous researchers.[10] In this study, limiting strength of the strengthened infilled frame has been successfully achieved in the test of Specimen IXFC. As seen in Fig. 9, a strain level of approximately 0.006 was achieved in both faces until the debonding and rupture of the CFRP cross overlays. These limit state values can be adopted in the development of design methodologies and structural models.

EFFECT OF FRP CONFIGURATION ON PERFORMANCE

The response of Specimen IX, which was the first CFRP-strengthened infill frame in the set, was mainly governed by

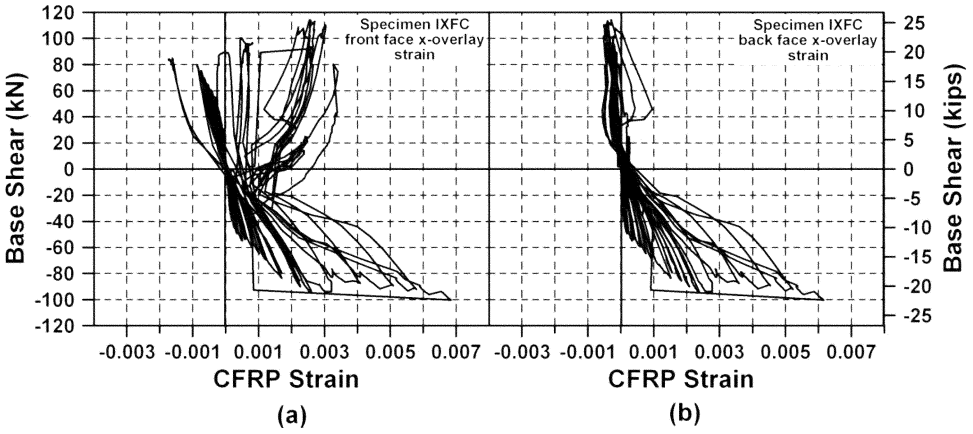

Fig. 9—CFRP strain response in cross overlay of Specimen IXFC: (a) front face—first-story panel; and (b) back face—first-story panel.

the efficiency of the strengthening scheme. Although cross-diagonal overlays enhanced the lateral load capacity of Specimen IXF with respect to Specimen IX, it was observed that the performance was appreciably affected by the capacity of the cross overlay anchor dowels providing proper connection to the surrounding frame and masonry infill. As observed in the comparable study conducted by METU (that is, Specimens SP-2 to SP-4), however, the governing failure mode was always the FRP buckling at the infill panel edges. In these studies, it was also concluded that the extension of the FRP (that is, in either the blanket or diagonal types of configuration) to the surrounding frame improved the behavior to some extent. It is clear that a cross overlay application scheme resulted in a more economical retrofitting scheme compared to a blanket-type application.

Applying CFRP flag sheets to the panel corners has been successfully employed to reduce the crushing of brick infill in the panel compression zones. In ITU's test campaign, flag sheets also worked favorably in all retrofitted configurations, indicating that this application has crucial role in preventing the corner crushing type of failure mode, stemming from the excessive compressive force demands in the infill corners. Another advantage of applied flag sheets along with the cross overlays anchored to the masonry infills may be the prevention of the out-of-plane movement of the infill panels by keeping them intact. At this point, the design and manufacturing of the special anchors made with CFRP materials gains a lot of importance in the prevention of premature local failures. For instance, in Specimen IXF, toward the peak load level, previously formed cracks at the foundation level widened suddenly and a rocking type of behavior was more pronounced, indicating a deficiency in the foundation anchorage detailing. Observations revealed that the problem of the lap splice in the columns was still governing the lateral load capacity and post-yield behavior. It is also noted in one of METU's tests (that is, Specimen SP-3) that the failure was triggered by the untimely failure of one anchor in the second-story columns.[10]

In addition to the CFRP overlays for confinement in the column lapped splice region, Specimen IXFC had vertical CFRP strips, assuring column reinforcing bar continuity between the first and second stories and between the foundation and first-story columns. The depth of the FRP anchor dowels in the foundation was increased from 80 to 120 mm (3.1 to 4.7 in.) in Specimen IXFC. The same retrofit scheme was used in the ITU tests with deeper anchorage lengths of 160 mm (6.3 in.) with the only difference being the direction of the anchor dowels used. In the ITU study, anchor locations were drilled vertically into the column, whereas in this study, a 45-degree inclination was employed (Fig. 2). To suppress the lap splice problem, CFRP strips were applied externally on the outer faces of the columns with an anchorage depth of 120 mm (4.7 in.). The CFRP amount was estimated based on the equivalent capacity of the longitudinal column bars close to the outer face of the column.

It is interesting to note that in ITU's tests (with 1/2-scale test specimens), different types of failure modes were observed, such as FRP diagonal ruptures in the first story along with the yielding of longitudinal reinforcement. On the other hand, in the METU tests, the failure modes were mainly governed by anchor failure and brittle shear failure of beam-column joints. Note that, although confinement was supplied in the plastic hinge zones, no flag sheets were applied in the METU study.

SUMMARY AND CONCLUSIONS

This paper summarizes the results of an experimental study on CFRP-strengthened hollow clay tile infilled RC frames. Specimens tested under reversed cyclic loading had the common deficiencies that are observed in practice. The following conclusions can be drawn based on the test results presented in this paper:

The proposed cross overlay CFRP strengthening scheme with flag sheets, special anchorage details, CFRP confinement, and CFRP continuity strips resulted in a significant response enhancement. Consecutive CFRP detailing from Specimens IX to IXFC had different levels of effectiveness on the frame behavior. From a global point of view, the masonry infills in the existing RC frames, formerly regarded as nonstructural elements, can successfully be transformed into structural walls. In this way, interstory drift control can be achieved until the elastic limits are exceeded through providing sufficient stiffness against seismic attacks. In Table 1, the initial stiffness increase due to the masonry infills can clearly be observed. Compared to the bare-frame Specimen B, the stiffness increased by almost 8 and 11 times in infill frame Specimen I and the last retrofitted specimen, Specimen IXFC, respectively. Due to the limited ductility achieved in the tests, however, elastic force limits and drift limits for serviceability issues can be implemented for the seismic retrofit design.

On the other hand, many improvements and observations are made regarding the local behavior. Whereas the failure pattern of Specimen IX was due to the corner crushing of the brick infill walls, this problem was solved in Specimen IXF by applying flag sheets and using deeper foundation dowels. As the last step, the deficiencies of Specimen IXF, such as the lap splice failure of the column longitudinal reinforcement and the inadequate CFRP anchor dowel length at the foundation level, were improved by using column confinement and externally applied CFRP continuity strips anchored to the frame foundation. It should be noted that system strengthening might result in a change in both the failure zone and the mechanism of the structure, as seen in Specimen IXFC.

In spite of the significant improvement observed in the lateral load-carrying capacity, the stiffness enhancement of the strengthened specimens was comparably low. The strength demand of the CFRP-strengthened brick-infilled RC frames will not significantly increase due to the small increase in lateral stiffness, whereas the capacity of the frames nearly doubled, as in the case of Specimen IXFC. In addition to strength enhancement, high energy dissipation capacity was also an advantage for the CFRP-strengthened specimens, especially Specimen IXFC. The degree of strengthening in the retrofitted specimens (referring to as-built infill frames) was 35%, 61%, and 65% for Specimens IX, IXF, and IXFC, respectively. In terms of energy dissipation capacity, Specimens IX and IXFC dissipated 2.8 and 3.6 times more energy compared to Specimen I.

The contribution of the infill walls strengthened with CFRP overlays to the seismic resistance of the existing structures is obvious. What is critical here is the reliance on a retrofit analysis and design that limits the story drift to an amount that would prevent any major degradation of the infill. The test results revealed that an interstory drift level of approximately 0.35 to 0.50% may be a limiting value preventing the CFRP-overlay-strengthened infill from degradation. To confirm these conclusions, further experimental and analytical studies should be carried out.

In addition to the enhancement in lateral load capacity, it may be concluded by visual inspection that the performance of the new strengthening scheme (Specimen IXFC) for the case with lap-spliced column reinforcement was the best among the specimens tested. Furthermore, the presence of the CFRP confinement overlays prevented the deterioration of concrete at the column ends, while rectangular CFRP flag sheets prevented the corner crushing of the infill. The failure of the CFRP confinement overlays at the first story, through peeling and delamination, occurred well beyond the lateral load capacity of the specimen. It is obvious that these effects led to an improved response under cyclic loading.

Last, but not least, although proposed retrofit solutions can be easily implemented with low invasiveness and minimum disruption to the building's functionality, workmanship in the design and application of CFRP overlays and special anchors to the surrounding frames is crucial in retrofitting practice. Disregarding this fact may lead to unforeseen disastrous consequences in the performance of the retrofitted structure during seismic action.

ACKNOWLEDGMENTS

The authors gratefully acknowledge the technical support of the Structures Laboratory in the Department of Civil Engineering at Bogazici University, Istanbul, Turkey, where all the experiments were conducted, and the financial support from the METU Civil Engineering Department Projects (NATO Scientific Affairs Division Grant No. SfP977231 and TUBITAK Grant No. YMAÜ-IÇTAG-I 575). The support of S. Y. Kimyasallari, who supplied the materials used in this study, is also gratefully acknowledged.

NOTATION

D_b = reinforcing bar diameter
E_e = modulus of elasticity of epoxy resin
E_f = modulus of elasticity of carbon fiber
f_c' = concrete compressive strength
f_e = tensile strength of epoxy resin
f_m' = mortar compressive strength
f_{uf} = tensile strength of carbon fiber
f_y = yield strength of reinforcing steel
f_{yw} = yield strength of transverse reinforcing steel
K^+ = initial stiffness of envelope curve for forward cycle
N = axial load on column
P_{cr} = lateral load level at which first crack was observed
P_{max} = maximum lateral load capacity of specimen
P_y = lateral load level at yield point of specimen
t_f = thickness of CFRP ply
w = width of CFRP strap
ε_{fu} = failure strain of CFRP

REFERENCES

1. Schwegler, G., "Masonry Construction Strengthened with Fiber Composites in Seismically Endangered Zones," *Proceedings of the Tenth European Conference on Earthquake Engineering*, Rotterdam, the Netherlands, 1995, pp. 2299-2303.

2. Weeks, J.; Sieble, F.; Hegemier, G.; and Kingsley, G., "The US-TCMMAR Full-Scale Five Story Masonry Research Building Test: Part V—Repair and Retest," *Research Report* No. SSRP-94/05, University of California, San Diego, San Diego, CA, 1994.

3. Ehsani, M. R.; Saadatmensh, H.; and Al-Saidy, A., "Shear Behavior of URM Retrofitted with FRP Overlays," *Journal of Composites for Construction*, ASCE, V. 3, No. 3, Feb. 1997, pp. 17-25.

4. Triantafillou, T. C., "Strengthening of Masonry Structures Using Epoxy Bonded FRP Laminates," *Journal of Composites for Construction*, ASCE, V. 2, No. 2, May 1998, pp. 96-104.

5. Li, T. et al., "Retrofit of Unreinforced Infill Masonry Walls with FRP," *Proceedings of the First International Conference on Composites in Construction*, Porto, Portugal, 2001, pp. 559-563.

6. Albert, M. L.; Elwi, A. E.; and Cheng, R. J. J., "Strengthening of Unreinforced Masonry Walls Using FRPs," *Journal of Composites for Construction*, ASCE, V. 5, No. 2, May 2001, pp. 76-84.

7. Hamoush, S. A. et al., "Out-of-Plane Strengthening of Masonry Walls with Reinforced Composites," *Journal of Composites for Construction*, ASCE, V. 5, No. 3, Aug. 2001, pp. 139-145.

8. Sugano, S., "State of the Art in Techniques for Rehabilitation of Buildings," *Eleventh World Conference on Earthquake Engineering*, *Paper* No. 2175, Acapulco, Mexico, 1996.

9. NATO Science for Peace Project SfP 977231, "Seismic Assessment and Rehabilitation of Existing Buildings," 2003, http://www.seru.metu.edu.tr/sfp977231/231_main.html.

10. Ozcebe, G. et al., "Strengthening of Brick-Infilled RC Frames with CFRP," *TUBITAK Structural Engineering Research Unit Report No. 2003-01*, Middle East Technical University, Ankara, Turkey, 2003.

11. Erol, G. et al., "Effective Strengthening of RC Frames with and without Lap Splice Problems," *Proceedings of the Eighth U.S. National Conference on Earthquake Engineering*, *Paper* No. 288, San Francisco, CA, 2006.

12. Saatcioglu, M.; Serrato, F.; and Foo, S., "Seismic Performance of Masonry Infill Walls Retrofitted with CFRP Sheets," *Seventh International Symposium on Fiber-Reinforced (FRP) Polymer Reinforcement for Concrete Structures*, SP-230, American Concrete Institute, Farmington Hills, MI, 2005, pp. 341-354.

13. Altin, S.; Anil, O.; Kara, M. E.; and Kaya, M., "An Experimental Study on Strengthening of Masonry Infilled RC Frames Using Diagonal CFRP Strips," *Composites Part B—Engineering*, V. 39, No. 4, Aug. 2008, pp. 680-693.

14. Akgüzel, U., "Seismic Retrofit of Brick Infilled R/C Frames with Lap Splice Problem in Columns," MSc thesis, Bogazici University, Istanbul, Turkey, 2003, 125 pp.

15. Chopra, A. K., *Dynamics of Structures, Theory and Applications to Earthquake Engineering*, Prentice Hall, Upper Saddle River, NJ, 2007, 876 pp.